

Upper Bounding GED via Transformations to LSAPE Based on Rings and Machine Learning

David B. Blumenthal, Sébastien Bougleux, Johann Gamper, Luc Brun

Abstract—The graph edit distance (GED) is a flexible distance measure which is widely used for inexact graph matching. Since its exact computation is \mathcal{NP} -hard, heuristics are used in practice. A popular approach is to obtain upper bounds for GED via transformations to the linear sum assignment problem with error-correction (LSAPE). Typically, local structures and distances between them are employed for carrying out this transformation, but recently also machine learning techniques have been used. In this paper, we formally define a unifying framework LSAPE-GED for transformations from GED to LSAPE. We introduce rings as a new kind of local structures that are able to capture a lot of information encoded in the input graphs at a low computational cost. Furthermore, we propose two new ring based heuristics RING and RING-ML , which instantiate LSAPE-GED using the traditional and the machine learning based approach for transforming GED to LSAPE, respectively. Extensive experiments show that using rings for upper bounding GED significantly improves the state of the art on datasets where most information resides in the graphs' topologies.

Index Terms—Graph Edit Distance, Graph Matching, Graph Similarity Search, Machine Learning



1 INTRODUCTION

LABELED graphs can be used for modeling various kinds of objects, such as chemical compounds, images, molecular structures, and many more. Because of this flexibility, labeled graphs have received increasing attention over the past years. One task researchers have focused on is the following: Given a database \mathcal{G} that contains labeled graphs, find all graphs $G \in \mathcal{G}$ that are sufficiently similar to a query graph H or find the k graphs from \mathcal{G} that are most similar to H [1], [2]. Being able to quickly answer graph similarity queries of this kind is crucial for the development of performant pattern recognition techniques in various application domains [3], such as keyword spotting in handwritten documents [4] and cancer detection [5].

For answering graph similarity queries, a distance measure between two labeled graphs G and H has to be defined. A very flexible, sensitive and therefore widely used measure is the graph edit distance (GED), which is defined as the minimum cost of an edit path between G and H [6]. An edit path is a sequence of graphs starting at G and ending at a graph that is isomorphic to H such that each graph on the path can be obtained from its predecessor by applying one of the following edit operations: adding or deleting an isolated node or an edge, and relabelling an existing node or edge. Each edit operation comes with an associated non-negative edit cost, and the cost of an edit path is defined as the sum of the costs of its edit operations. GED inherits metric properties from the underlying edit costs [7]. For instance, if \mathcal{G} is the domain of graphs with real-valued node and edge labels and the edit costs are defined as the Euclidean distances between the labels, then GED is a metric on \mathcal{G} .

GED is mainly used in settings where we have to answer fine-grained similarity queries for (possibly very many) rather small graphs. For instance, this is the case in keyword spotting in handwritten documents, cancer detection, and drug discovery [3]. If the graphs are larger, faster approaches such as embedding the graphs into vector spaces and then comparing their vector representations are employed [1], [2]. The drawback of these faster techniques is that a substantial part of the local information encoded in the original graphs is lost when embedding them into vector spaces. Whenever this information loss is intolerable, it is advisable to compare the graphs directly in the graph space—and one of the most commonly used distance measure for doing so is GED.

1.1 Related Work

Computing GED is a very difficult problem. It has been shown that the problem of computing GED is \mathcal{NP} -hard even for uniform edit costs [8], and \mathcal{APX} -hard for metric edit costs [9]. Even worse: since, by definition of GED, it holds that $\text{GED}(G, H) = 0$ just in case G and H are isomorphic, approximating GED within any approximation ratio is \mathcal{GT} -hard. These theoretical complexities are mirrored by the fact that, in practice, no available exact algorithm can reliably compute GED on graphs with more than 16 nodes [10].

Because of GED's complexity, research has mainly focused on heuristics. The development of heuristics was particularly triggered by the presentation of the algorithms BP [11] and STAR [8], which use transformations to the linear sum assignment problem with error correction (LSAPE)—a variant of the linear sum assignment problem (LSAP) where rows and columns may also be inserted and deleted—to compute upper bounds for GED. BP and STAR work as follows: First, the nodes of the input graphs are associated with local structures composed of branches (BP) or stars (STAR), respectively. The branch of a node is defined as the node itself together with its incident edges, whereas the star additionally

- D. B. Blumenthal and J. Gamper are with the Faculty of Computer Science, Free University of Bozen-Bolzano, Bolzano, Italy.
E-mail: david.blumenthal@inf.unibz.it, gamper@inf.unibz.it
- S. Bougleux and L. Brun are with the Normandie Université, UNICAEN, ENSICAEN, CNRS, GREYC, Caen, France.
E-mail: bougleux@unicaen.fr, luc.brun@ensicaen.fr

contains the incident edges’ terminal nodes. Then, suitable distance measures between, respectively, branches and stars are used to populate instances of LSAP whose rows and columns correspond to the input graphs’ nodes. Finally, the solution of the LSAP instance is interpreted as an edit path whose cost is returned as upper bound for GED.

Following BP and STAR, many similar algorithms have been proposed. Like BP, the algorithms BRANCH-UNI [12], BRANCH-FAST [13], and BRANCH [13] use branches as local structures, but use slightly different distance measures between the branches that allow to also derive lower bounds. The main disadvantage of these algorithms as well as of BP and STAR is that, due to the very narrow locality of the local structures, they yield unsatisfactorily loose upper bounds on datasets where the nodes only carry little information and most information instead resides in the graphs’ topologies.

In order to produce tight upper bounds even if there is little information on the nodes, the algorithms SUBGRAPH [14] and WALKS [15] associate the nodes with larger local structures — namely, subgraphs of fixed radiuses and sets of walks of fixed lengths. The drawback of SUBGRAPH is that it runs in polynomial time only if the input graphs have constantly bounded maximum degrees. WALKS avoids this blowup, but only models constant edit costs and uses local structures that may contain redundant information due to multiple inclusions of nodes and edges. It has also been suggested to tighten the upper bounds by incorporating node centrality measures into the LSAP instances [16], [17].

Recently, two machine learning based heuristics for GED have been proposed. The algorithm PREDICT [18] calls BP to compute an LSAP instance and uses statistics of the LSAP instance to define feature vectors for all node assignments. PREDICT then trains a support vector classifier (SVC) to predict if a node edit assignment is contained in an optimal edit path. The algorithm NGM [19] defines feature vectors of node substitutions in terms of the input graphs’ node labels and node degrees. Given a set of optimal edit paths, NGM trains a deep neural network (DNN) to output a value close to 0 if the substitution is predicted to be in an optimal edit path, and close to 1, otherwise. The output is used to populate an instance of the linear sum assignment problem (LSAP), whose solution induces an upper bound for GED. NGM does not support node insertions and deletions and can hence be used only for equally sized graphs. Moreover, it ignores edge labels and assumes that the node labels are real-valued vectors. PREDICT works for general graphs but does not yield an upper bound for GED.

Not all heuristics for GED build upon transformations to LSAP. Most notably, various algorithms have been proposed that improve an initially computed or randomly generated upper bound by using variants of local search [8], [20], [21], [22], [23], [24], [25], [26]. These methods are much slower than LSAP based heuristics but yield significantly tighter upper bounds. Moreover, they can be set up to use LSAP based heuristics for initialization. Hence, they should not be viewed as competitors to LSAP based heuristics.

1.2 Contributions

In this paper, we formally describe a paradigm LSAP-GED that generalizes all existing transformations from GED

to LSAP. While classical instantiations of LSAP-GED such as BP, STAR, BRANCH-UNI, BRANCH-FAST, BRANCH, SUBGRAPH, and WALKS use local structures and distance measures between them for the transformation, we also suggest a new, machine learning based approach inspired by the algorithms PREDICT and NGM: During training, feature vectors for all possible node assignments are constructed and a machine learning framework is trained to output a value close to 0 if a node assignment is predicted to be contained in an optimal edit path, and a value close to 1, otherwise. At runtime, the output of the machine learning framework is fed into an LSAP instance.

As mentioned above, PREDICT and NGM use SVCs or DNNs as their machine learning frameworks. They hence require training data that consists of node assignments some of which are and some of which are not contained in optimal edit paths. We argue that constructing such training data in a clean way is computationally infeasible. In order to overcome this problem, we suggest to use one class support vector machines (1-SVM) instead of SVCs and DNNs.

Next, we present a new kind of local structures — namely, rings of fixed sizes. Rings are sequences of disjoint node and edge sets at fixed distances from a root node. As the subgraph and walks structures used by SUBGRAPH and WALKS, rings are designed to capture more topological information than the local structures used by the baseline approaches BP and STAR. The advantage w.r.t. subgraphs is that rings can be processed in polynomial time. The advantage w.r.t. walks is that rings model general edit costs and avoid redundancies due to multiple inclusions of nodes and edges.

Subsequently, we propose RING and RING-ML, two instantiations of LSAP-GED that make crucial use of rings. RING adopts the classical approach, i.e., carries out the transformation via a suitably defined ring distance measure. In contrast to that, RING-ML uses rings to construct feature vectors for the node assignments and then uses machine learning techniques to carry out the transformation. An extensive empirical evaluation shows that, among all instantiations of LSAP-GED, RING produces the tightest upper bound for GED, and that the machine learning based instantiation RING-ML shows very promising potential, too. In sum, our paper contains the following contributions:

- We formally define the paradigm LSAP-GED, formalize the classical, local structure distance based approach for transforming GED to LSAP, and show how to use machine learning techniques for this purpose (Section 3).
- We argue that one should use 1-SVMs instead of classifiers such as DNNs or SVCs if one wants to use machine learning for transforming GED to LSAP (Section 3).
- We introduce rings, a new kind of local structures to be used by instantiations of LSAP-GED that aim at computing tight upper bounds also if most information resides in the graphs’ topologies rather than in the node labels (Section 4).
- We present two new LSAP-GED instantiations RING and RING-ML (Section 5).
- We empirically evaluate the new algorithms (Section 6).

TABLE 1
Notation Table

syntax	semantic
\mathfrak{G}	graphs on label alphabets Σ_V and Σ_E
\mathfrak{J}	graph-node incidences in \mathfrak{G}
\mathfrak{A}	node assignments between graphs in \mathfrak{G}
$c_V(\ell_V^G(u), \ell_V^H(u))$	cost of substituting $u \in V^G$ by $v \in V^H$
$c_E(\ell_E^G(e), \ell_E^H(f))$	cost of substituting $e \in E^G$ by $f \in E^H$
$c_V(\ell_V^G(u), \epsilon)$	cost of deleting $u \in V^G$
$c_E(\ell_E^G(e), \epsilon)$	cost of deleting $e \in E^G$
$c_V(\epsilon, \ell_V^H(u))$	cost of inserting $v \in V^H$
$c_E(\epsilon, \ell_E^H(f))$	cost of inserting $f \in E^H$
$\Pi(G, H)$	node maps between graphs G and H
$c(\pi)$	node map π 's induced edit cost
$\Pi(\mathbf{C})$	feasible solutions for LSAPE instance \mathbf{C}

This paper extends the results presented in [27], where we informally described LSAPE-GED, introduced rings, and presented and preliminarily evaluated RING. In particular, the following contributions are new: formal definition of LSAPE-GED, the use of machine learning techniques in general and 1-SVMs in particular for transforming GED to LSAPE, the algorithm RING-ML, and additional experiments.

The remainder of the paper is organized as follows: In Section 2, we introduce concepts and notations. In Sections 3 to 6, our contributions are presented. Section 7 concludes the paper.

2 PRELIMINARIES

We consider undirected labeled graphs $G = (V^G, E^G, \ell_V^G, \ell_E^G)$ from a domain of graphs \mathfrak{G} . V^G and E^G are sets of nodes and edges, Σ_V and Σ_E are label alphabets, and $\ell_V^G : V^G \rightarrow \Sigma_V$ and $\ell_E^G : E^G \rightarrow \Sigma_E$ are labeling functions. $\mathfrak{J} := \{(G, u) \mid G \in \mathfrak{G} \wedge u \in (V^G \cup \epsilon)\}$ is the set of all graph-node incidences and $\mathfrak{A} := \{(G, H, u, v) \mid (G, u) \in \mathfrak{J} \wedge (H, v) \in \mathfrak{J} \wedge u \neq \epsilon \vee v \neq \epsilon\}$ is the set of all node assignments. The symbol ϵ denotes dummy nodes and edges as well as their labels. For each $N \in \mathbb{N}_{\geq 1}$, we define $[N] := \{n \in \mathbb{N}_{\geq 1} \mid n \leq N\}$.

An edit path from a graph G to a graph H is a sequence of edit operations that transforms G into H . There are six edit operations: Substituting a node or and edge from G by a node or an edge from H , deleting an isolated node or an edge from G , and inserting an isolated node or an edge between two existing nodes into H . Each edit operation o comes with an edit cost $c(o)$ defined in terms of edit cost functions $c_V : \Sigma_V \cup \{\epsilon\} \times \Sigma_V \cup \{\epsilon\} \rightarrow \mathbb{R}_{\geq 0}$ and $c_E : \Sigma_E \cup \{\epsilon\} \times \Sigma_E \cup \{\epsilon\} \rightarrow \mathbb{R}_{\geq 0}$ (cf. Table 1), which respect $c_V(\alpha, \alpha) = 0$ and $c_E(\beta, \beta) = 0$ for all $\alpha \in \Sigma_V \cup \{\epsilon\}$ and all $\beta \in \Sigma_E \cup \{\epsilon\}$. The cost of an edit path $P = (o_i)_{i=1}^r$ is defined as $c(P) := \sum_{i=1}^r c(o_i)$.

Definition 1 (GED). Let $\Psi(G, H)$ be the set of all edit paths from a graph G to a graph H . Then graph edit distance is defined as $\text{GED}(G, H) := \min_{P \in \Psi(G, H)} c(P)$.

Definition 1 is very intuitive but impractical for algorithmic purposes, because for recognizing an edit path as such, one has to solve the graph isomorphism problem. Thus, algorithms for GED use an alternative definition based on the concept of error-correcting matchings [6], also called node

maps [10], [23]. In this paper, we use the term “node map”. Also note that metric properties of the edit costs propagate to GED [7]. Since the edit costs which are typically employed for commonly used benchmark datasets are symmetric [28], [29], in this paper, we therefore speak of the graph edit distance “between” two graphs G and H .

Definition 2 (Node Map). Let G and H be graphs. A relation $\pi \subseteq (V^G \cup \{\epsilon\}) \times (V^H \cup \{\epsilon\})$ is called node map between G and H if and only if $|\{v \mid v \in (V^H \cup \{\epsilon\}) \wedge (u, v) \in \pi\}| = 1$ holds for all $u \in V^G$ and $|\{u \mid u \in (V^G \cup \{\epsilon\}) \wedge (u, v) \in \pi\}| = 1$ holds for all $v \in V^H$. We write $\pi(u) = v$ just in case $(u, v) \in \pi$ and $u \neq \epsilon$, and $\pi^{-1}(v) = u$ just in case $(u, v) \in \pi$ and $v \neq \epsilon$. $\Pi(G, H)$ denotes the set of all node maps between G and H .

A node map $\pi \in \Pi(G, H)$ specifies for all nodes $u \in V^G$ and $v \in V^H$ and all edges $e = (u_1, u_2) \in E^G$ and $f = (v_1, v_2) \in E^H$ if they are substituted, deleted, or inserted: If $\pi(u) = v$, the node u is substituted by v ; if $\pi(u) = \epsilon$, u is deleted; and if $\pi^{-1}(v) = \epsilon$, v is inserted. Similarly, if $(\pi(u_1), \pi(u_2)) = (v_1, v_2)$, the edge e is substituted by f ; if $(\pi(u_1), \pi(u_2)) \notin E^H$, e is deleted; and if $(\pi^{-1}(v_1), \pi^{-1}(v_2)) \notin E^G$, f is inserted. A node map $\pi \in \Pi(G, H)$ hence induces an edit path from G to H . It has been shown that, for computing GED, it suffices to consider edit paths induced by node maps [6], [10], [23], [30].

Theorem 1 (Alternative Definition of GED). Let G and H be graphs and $c(\pi)$ be the cost of the edit path induced by a node map $\pi \in \Pi(G, H)$. Then, under mild constraints on the edit costs that can be assumed to hold w.l.o.g., it holds that $\text{GED}(G, H) = \min_{\pi \in \Pi(G, H)} c(\pi)$.

Since node maps are much easier objects to work with than edit paths, Theorem 1 renders GED algorithmically accessible. In particular, it implies that each node map induces an upper bound for GED. This observation is used by approximative methods for GED to heuristically compute a node map that induces a tight upper bound. For finding such a node map, many heuristics [8], [11], [12], [13], [14], [15], [16], [17] use the linear sum assignment problem with error correction (LSAPE) [31], [32] — although usually not under this name, since LSAPE was formalized after the presentation of most of these heuristics.

Definition 3 (LSAPE). Let $\mathbf{C} = (c_{i,k}) \in \mathbb{R}^{(n+1) \times (m+1)}$ be a matrix with $c_{n+1, m+1} = 0$. A relation $\pi \subseteq [n+1] \times [m+1]$ is a feasible LSAPE solution for \mathbf{C} , if and only if $|\{k \mid k \in [m+1] \wedge (i, k) \in \pi\}| = 1$ holds for all $i \in [n]$ and $|\{i \mid i \in [n+1] \wedge (i, k) \in \pi\}| = 1$ holds for all $k \in [m]$. We write $\pi(i) = k$ if $(i, k) \in \pi$ and $i \neq n+1$; and $\pi^{-1}(k) = i$ if $(i, k) \in \pi$ and $k \neq m+1$. The set of all feasible LSAPE solutions for \mathbf{C} is denoted by $\Pi(\mathbf{C})$. The cost of a feasible solution $\pi \in \Pi(\mathbf{C})$ is defined as $\mathbf{C}(\pi) := \sum_{(i,k) \in \pi} c_{i,k}$. The set of all optimal LSAPE solutions for \mathbf{C} is defined as $\Pi^*(\mathbf{C}) := \arg \min_{\pi \in \Pi(\mathbf{C})} \mathbf{C}(\pi)$.

An optimal LSAPE solution $\pi \in \Pi^*(\mathbf{C})$ can be computed in $O(\min\{n, m\}^2 \max\{n, m\})$ time [32]. Once one optimal solution has been found, for each $s \in [\Pi^*(\mathbf{C})]$, a solution set $\Pi_s^*(\mathbf{C}) \subseteq \Pi^*(\mathbf{C})$ of size s can be enumerated in $O(nm\sqrt{n+m} + s \log(n+m))$ time [33]. Greedy suboptimal solutions can be computed in $O(nm)$ time [34].

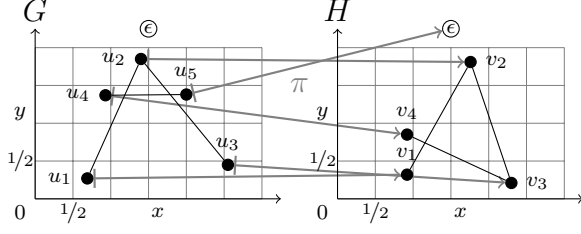


Fig. 1. Two graphs G and H from the LETTER dataset and a node map π between them.

Node maps and feasible solutions for LSAPE are closely related. Consider graphs G and H and an LSAPE instance $\mathbf{C} \in \mathbb{R}^{(|V^G|+1) \times (|V^H|+1)}$. Definition 2 and Definition 3 imply that we can identify the set $\Pi(G, H)$ of all node maps between G and H with the set $\Pi(\mathbf{C})$ of all feasible LSAPE solutions for \mathbf{C} : For all $i \in [|V^G|]$ and all $k \in [|V^H|]$, we associate \mathbf{C} 's i^{th} row with the node $u_i \in V^G$ and \mathbf{C} 's k^{th} column with the node $v_k \in V^H$. The last row and the last column of \mathbf{C} are associated with the dummy node ϵ . Then, each feasible LSAPE solution π for \mathbf{C} yields an upper bound for $\text{GED}(G, H)$ —namely, the cost $c(\pi)$ of the edit path induced by π 's interpretation as a node map.

Example 1 (Illustration of Most Important Definitions).

Consider the graphs G and H shown in Figure 1. G and H are taken from the LETTER dataset and represent distorted letter drawings [35]. Their nodes are labeled with two-dimensional, non-negative Euclidean coordinates. Edges are unlabeled. Hence, we have $\Sigma_V = \mathbb{R}_{\geq 0} \times \mathbb{R}_{\geq 0}$ and $\Sigma_E = \{1\}$. In [28], it is suggested that the edit cost functions c_V and c_E for LETTER should be defined as follows: $c_E(1, \epsilon) := c_E(\epsilon, 1) := 0.425$, $c_V(\alpha, \alpha') := 0.75 \|\alpha - \alpha'\|$, and $c_V(\alpha, \epsilon) := c_V(\epsilon, \alpha) := 0.675$ for all node labels $\alpha, \alpha' \in \Sigma_V$, where $\|\cdot\|$ is the Euclidean norm. Now consider the node map $\pi \in \Pi(G, H)$ shown in Figure 1. It induces the following edit operations: The nodes u_i have to be substituted by the nodes v_i , for all $i \in [4]$. The node u_5 has to be deleted. The edges (u_1, u_2) and (u_2, u_3) have to be substituted by the edges (v_1, v_2) and (v_2, v_3) , respectively. The edge (u_4, u_5) has to be deleted. The edge (v_3, v_4) has to be inserted. By summing the induced edit costs, we obtain that π 's induced edit path has cost $c(\pi) = 2.574$, which implies $\text{GED}(G, H) \leq 2.574$.

3 LSAPE BASED UPPER BOUNDS FOR GED

In this section, we present the paradigm LSAPE-GED, show that existing LSAPE based approaches for upper bounding GED are instances of LSAPE-GED, and present a new machine learning technique to create LSAPE instances. We also identify a problem that occurs if classifiers such as SVCs or DNNs are used for creating the LSAPE instances, and suggest that one should resort to 1-SVMs to overcome it.

3.1 Overall Structure of the Paradigm LSAPE-GED

Figure 2 shows how to use LSAPE for upper bounding GED: Given two graphs G and H , first an LSAPE instance $\mathbf{C} \in \mathbb{R}^{(|V^G|+1) \times (|V^H|+1)}$ is constructed. Different strategies can be used for the construction, which are detailed in

Section 3.2 and Section 3.3. Subsequently, existing LSAPE based heuristics call a greedy or an optimal solver to compute an LSAPE solution $\pi \in \Pi(\mathbf{C})$ and interpret π as a node map whose induced edit cost is returned as an upper bound for GED. Alternatively, given a constant $s > 1$, we suggest to use an optimal LSAPE solver in combination with the enumeration procedure in [33] in order to generate a set $\Pi_s^*(\mathbf{C}) \subseteq \Pi^*(\mathbf{C})$ of optimal LSAPE solutions with size $|\Pi_s^*(\mathbf{C})| = \min\{s, |\Pi^*(\mathbf{C})|\}$. A tightened upper bound for GED can then be obtained by minimizing the induced edit cost over the solution set $\Pi_s^*(\mathbf{C})$. Using the enumeration procedure in [33] to compute solution sets $\Pi_s^*(\mathbf{C})$ with $s > 1$ was suggested in [24], where $\Pi_s^*(\mathbf{C})$'s elements are used as initial solutions for a refinement algorithm based on local search. However, to the best of our knowledge, this technique has never been used for tightening the upper bounds produced by LSAPE based heuristics.

3.2 Classical Strategy for Populating the LSAPE Instance

Classical instantiations of the paradigm LSAPE-GED construct the LSAPE instance \mathbf{C} by using local structures rooted at the nodes and distance measures between them. Formally, they define local structure functions $\mathcal{S} : \mathcal{I} \rightarrow \mathcal{S}$ that map graph-nodes incidences to elements of a suitably defined space of local structures \mathcal{S} , and distance measures $d_{\mathcal{S}} : \mathcal{S} \times \mathcal{S} \rightarrow \mathbb{R}_{\geq 0}$ for the local structures. Given input graphs G and H on node sets $V^G = \{u_1, \dots, u_{|V^G|}\}$ and $V^H = \{v_1, \dots, v_{|V^H|}\}$, the LSAPE instance $\mathbf{C} \in \mathbb{R}^{(|V^G|+1) \times (|V^H|+1)}$ is then defined as

$$\begin{aligned} c_{i,k} &:= d_{\mathcal{S}}(\mathcal{S}(G, u_i), \mathcal{S}(H, v_k)), \\ c_{i,|V^H|+1} &:= d_{\mathcal{S}}(\mathcal{S}(G, u_i), \mathcal{S}(H, \epsilon)), \text{ and} \\ c_{|V^G|+1,k} &:= d_{\mathcal{S}}(\mathcal{S}(G, \epsilon), \mathcal{S}(H, v_k)), \end{aligned}$$

for all $(i, k) \in [|V^G|] \times [|V^H|]$. This classical strategy for populating \mathbf{C} is adopted by the existing heuristics BP [11], STAR [8], BRANCH-UNI [12], BRANCH [13], BRANCH-FAST [13], WALKS [15], and SUBGRAPH [14], as well as by the algorithm RING proposed in this paper (Section 5.1). Also the node centrality based heuristics [16], [17] can be subsumed under this model; here, the “local structures” are simply the nodes’ centralities.

Example 2 (Illustration of Classical Instantiations of LSAPE-GED).

Consider the following very simple classical instantiation of LSAPE-GED that uses the input graphs’ node labels as its local structures and the node edit costs as the local structure distances. In other words, our toy instantiation of LSAPE-GED sets $\mathcal{S} := \mathcal{I}$ and $d_{\mathcal{S}} := c_V$. Again consider the graphs G and H shown in Figure 1 and assume that the node edit costs c_V are defined as detailed in Example 1. Figure 3 shows the obtained LSAPE instance \mathbf{C} . Its optimal solution $\pi := \{(i, i) \mid i \in [5]\}$ selects the bold-faced cells of \mathbf{C} and corresponds to the node map shown in Figure 1. Its LSAPE cost is therefore $\mathbf{C}(\pi) = 1.774$, while the induced upper bound for GED equals $c(\pi) = 2.574$.

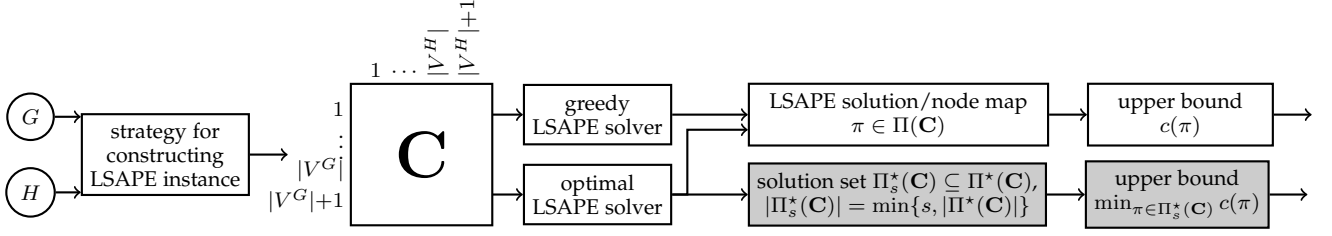


Fig. 2. The paradigm LSAPG-GED . Our alternative solution strategy is displayed in grey.

	1	2	3	4	5
1	0.177	1.406	1.208	0.468	0.675
2	1.203	0.272	1.403	0.832	0.675
3	1.226	1.180	0.260	1.259	0.675
4	0.788	0.705	1.346	0.390	0.675
5	1.135	0.369	0.906	0.902	0.675
6	0.675	0.675	0.675	0.675	0

Fig. 3. LSAPG instance \mathbf{C} for the graphs shown in Figure 1 constructed by the toy instantiation of LSAPG-GED described in Example 2. Bold-faced cells correspond to the node assignments contained in optimal solution.

3.3 Machine Learning Based Strategy for Populating the LSAPG Instance

3.3.1 General Strategy

Instead of using local structures, LSAPG instances can be constructed with the help of feature vectors associated to good and bad node assignments. This strategy is inspired by the existing algorithms PREDICT [18] and NGM [19]. However, as detailed in Section 3.3.3 below, both PREDICT and NGM fall short of completely instantiating it.

Definition 4 (Good and Bad Node Assignments). A node assignment $(G, H, u, v) \in \mathcal{A}$ is called good if and only if it is contained in an optimal node map, i.e., if there is a node map $\pi \in \Pi(G, H)$ with $c(\pi) = \text{GED}(G, H)$ and $(u, v) \in \pi$. The set of all good node assignments is denoted by \mathcal{A}^* . Node assignments contained in $\mathcal{A} \setminus \mathcal{A}^*$ are called bad.

If machine learning techniques are used for populating the LSAPG instance $\mathbf{C} \in \mathbb{R}^{(|V^G|+1) \times (|V^H|+1)}$, in a first step, feature vectors $\mathcal{F} : \mathcal{A} \rightarrow \mathbb{R}^d$ for the node assignments have to be defined. Subsequently, a function $p^* : \mathbb{R}^d \rightarrow [0, 1]$ has to be learned, which maps feature vectors $\mathbf{x} \in \mathcal{F}[\mathcal{A}^*]$ to large values and feature vectors $\mathbf{x} \in \mathcal{F}[\mathcal{A} \setminus \mathcal{A}^*]$ to small values. Informally, $p^*(\mathbf{x})$ can be viewed as an estimate of the probability that a feature vector $\mathbf{x} \in \mathcal{F}[\mathcal{A}]$ is associated to a good node map. Once p^* has been learned, \mathbf{C} is defined as

$$\begin{aligned} c_{i,k} &:= 1 - p^*(\mathcal{F}(G, H, u_i, v_k)), \\ c_{i,|V^H|+1} &:= 1 - p^*(\mathcal{F}(G, H, u_i, \epsilon)), \text{ and} \\ c_{|V^G|+1,k} &:= 1 - p^*(\mathcal{F}(G, H, \epsilon, v_k)), \end{aligned}$$

for all $(i, k) \in [|V^G|] \times [|V^H|]$.

3.3.2 Choice of Machine Learning Technique

For learning the probability estimate p^* , several strategies can be adopted. Given a set \mathcal{G} of training graphs, one can

mimic PREDICT and compute optimal node maps $\pi_{G,H}$ for the training graphs. These node maps can be used to generate training data

$$\mathcal{T} := \{(\mathcal{F}(G, H, u, v), \delta_{(u,v) \in \pi_{G,H}}) \mid (G, H, u, v) \in \mathcal{A}[\mathcal{G}]\},$$

where $\delta_{\text{true}|\text{false}}$ maps true to 1 and false to 0, and $\mathcal{A}[\mathcal{G}]$ is the restriction of \mathcal{A} to the graphs contained in \mathcal{G} . Finally, a kernelized SVC with probability estimates [36] can be trained on \mathcal{T} . Alternatively, one can proceed like NGM , i.e., use \mathcal{T} to train a fully connected feedforward DNN with output from $[0, 1]$, and define p^* as the output of the DNN.

The drawback of these approaches is that some feature vectors contained in \mathcal{T} are incorrectly labeled as bad if there is more than one optimal node map. Assume that, for training graphs G and H , there are two optimal node maps $\pi_{G,H}$ and $\pi'_{G,H}$, and that the exact algorithm used for generating \mathcal{T} computes $\pi_{G,H}$. Let (G, H, u, v) be a node assignment such that (u, v) is contained in $\pi'_{G,H} \setminus \pi_{G,H}$. According to Definition 4, (G, H, u, v) is a good node assignment, but in \mathcal{T} , its feature vector $\mathbf{x} := \mathcal{F}(G, H, u, v)$ is labeled as bad.

A straightforward but computationally infeasible way to tackle this problem is to compute all optimal node maps for the training graphs. Instead, we suggest to train a one class support vector machine (1-SVM) [37] with RBF kernel to estimate the support of the feature vectors associated to good node maps. This has the advantage that, given a set \mathcal{G} of training graphs and initially computed optimal node maps $\pi_{G,H}$ for all $G, H \in \mathcal{G}$, we can use training data

$$\mathcal{T}^* := \{\mathcal{F}(G, H, u, v) \mid (G, H, u, v) \in \mathcal{A}[\mathcal{G}] \wedge (u, v) \in \pi_{G,H}\}$$

which contains only feature vectors associated to good node assignments and is hence correct even if there are multiple optimal node maps.

For the definition of p^* , recall that the decision function of a trained 1-SVM with RBF kernel is $\text{sgn}(h(\mathbf{x}))$, where $h(\mathbf{x}) = [\sum_{i=1}^{|\mathcal{T}^*|} \alpha_i \exp(-\gamma \|\mathbf{x}^i - \mathbf{x}\|_2^2)] - \rho$, α_i is the dual variable associated to the training vector $\mathbf{x}^i \in \mathcal{T}^*$, ρ defines the separating hyperplane in the feature space induced by the RBF kernel, and $\gamma > 0$ is a tuning parameter.

Remark 1 (Properties of 1-SVM). Let (α, ρ) be a 1-SVM with RBF kernel and tuning parameter γ that has been trained on data \mathcal{T}^* . Then $h(\mathbf{x}) \in (-\rho, \mathbf{1}^\top \alpha - \rho)$ holds for all $\mathbf{x} \in \mathbb{R}^d$, and $\mathbf{x} \mapsto (\gamma/\pi)^{d/2} (\mathbf{1}^\top \alpha)^{-1} (h(\mathbf{x}) + \rho)$ is the density function of the multivariate Gaussian mixture model $\mathcal{M}(\alpha, \gamma) := \sum_{i=1}^{|\mathcal{T}^*|} (\mathbf{1}^\top \alpha)^{-1} \alpha_i \mathcal{N}(\mathbf{0}, (2\gamma)^{-1} \mathbf{I})$ for the feature vectors $\mathcal{F}[\mathcal{A}^*]$ associated to good node assignments.

Remark 1 tells us how to transform the output of a trained

1-SVM into a probability estimate p^* . We simply define $p^*(\mathbf{x})$ as the likelihood of the feature vector \mathbf{x} under the model $\mathcal{M}(\alpha, \gamma)$ learned by the 1-SVM:

$$p^*(\mathbf{x}) := (\gamma/\pi)^{d/2} (\mathbf{1}^\top \alpha)^{-1} (h(\mathbf{x}) + \rho)$$

3.3.3 NGM and PREDICT in the Context of the General Strategy

We conclude this section by briefly summarizing why the existing heuristics NGM and PREDICT fail to fully instantiate the machine learning based transformation strategy described above. There are two problems with NGM: Firstly, its feature vectors are defined only for graphs whose node labels are real-valued vectors. Secondly, no feature vectors for node deletions and insertions can be constructed. This implies that NGM cannot populate the last row and the last column of its LSAP instance and can hence be used only for graphs whose optimal node maps are known upfront not to contain node insertions or deletions. Unlike NGM, PREDICT defines feature vectors that cover node deletions and insertions and are defined for general node and edge labels. However, PREDICT is designed to predict if a node assignment is good rather than to use the decision value for populating an LSAP instance. That is, instead of learning a probability estimate $p^* : \mathbb{R}^d \rightarrow [0, 1]$, PREDICT uses a kernelized SVC without probability estimates to learn a decision function $f^* : \mathbb{R}^d \rightarrow \{0, 1\}$ which maps feature vectors $\mathbf{x} \in \mathcal{F}[\mathfrak{A}^*]$ to 1 and feature vectors $\mathbf{x} \in \mathcal{F}[\mathfrak{A} \setminus \mathfrak{A}^*]$ to 0.

4 RINGS AS LOCAL STRUCTURES

In this section, we introduce rings of size L as a new kind of local structures. Subsequently, we show how to construct them. As mentioned above, rings are similar to the subgraph and walks structures used by SUBGRAPH and WALKS in that they capture more topological information than the local structures used by the baseline approaches BP, STAR, BRANCH-UNI, and BRANCH. They are hence designed to be used by instantiations of LSAP-GED that aim at computing tight upper bounds also on datasets where most information resides in the graphs' topologies. The advantage of rings w. r. t. subgraphs is that rings can be processed in polynomial time, while comparing local subgraphs is polynomial only on graphs with constantly bounded maximum degrees. The advantage of rings w. r. t. walks is that rings model general edit costs and avoid redundancies due to multiple inclusions of nodes and edges.

4.1 Rings: Definition

We define the rings rooted at the nodes of a graph G as L -sized sequences of layers $\mathcal{L}^G = (N^G, OE^G, IE^G)$, where $N^G \subseteq V^G$ is a subset of the nodes, and $OE^G, IE^G \subseteq E^G$ are subsets of the edges of G . Formally, the space of all L -sized rings for graphs from a domain \mathfrak{G} is defined as $\mathfrak{R}_L := \{(\mathcal{L}_l)_{l=0}^{L-1} \mid \mathcal{L}_l \in \bigcup_{G \in \mathfrak{G}} \mathfrak{L}(G)\}$, where $\mathfrak{L}(G) := \mathcal{P}(V^G) \times \mathcal{P}(E^G) \times \mathcal{P}(E^G)$. Next, we specify a function $\mathcal{R}_L : \mathfrak{I} \rightarrow \mathfrak{R}_L$ which maps a graph-node incidence (G, u) to a ring of size L . For this, we need some terminology: The distance $d_V^G(u, u')$ between two nodes $u, u' \in V^G$ is defined as the number of edges on a shortest path connecting them or as ∞ if they are in different connected components of G .

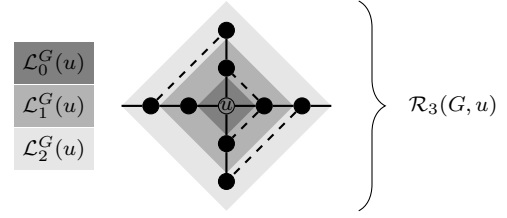


Fig. 4. Visualization of Definition 5. Inner edges are dashed, outer edges are solid. Layers are displayed in different shades of grey.

The eccentricity of a node $u \in V^G$ and the diameter of a graph G are defined as $e_V^G(u) := \max_{u' \in V^G} d_V^G(u, u')$ and $\text{diam}(G) := \max_{u \in V^G} e_V^G(u)$, respectively.

Definition 5 (Rings, Layers, Outer and Inner Edges). Given a constant $L \in \mathbb{N}_{>0}$, the function $\mathcal{R}_L : \mathfrak{I} \rightarrow \mathfrak{R}_L$ maps a graph-node incidence (G, u) to the ring $\mathcal{R}_L(G, u) := (\mathcal{L}_l^G(u))_{l=0}^{L-1}$ rooted at u in G (Figure 4). For the dummy node ϵ , we define $\mathcal{R}_L(G, \epsilon) := ((\emptyset, \emptyset, \emptyset))_{l=0}^{L-1}$. For all other nodes u , $\mathcal{L}_l^G(u) := (N_l^G(u), OE_l^G(u), IE_l^G(u))$ denotes the l^{th} layer rooted at u in G , where:

- 1) $N_l^G(u) := \{u' \in V^G \mid d_V^G(u, u') = l\}$ is the set of nodes at distance l of u .
- 2) $IE_l^G(u) := E^G \cap (N_l^G(u) \times N_l^G(u))$ is the set of inner edges connecting two nodes in the l^{th} layer.
- 3) $OE_l^G(u) := E^G \cap (N_l^G(u) \times N_{l+1}^G(u))$ is the set of outer edges connecting a node in the l^{th} layer to a node in the $(l+1)^{\text{th}}$ layer.

It is easy to see that the ring $\mathcal{R}_1(G, u)$ of a node $u \in V^G$ corresponds to the branch structure used by the LSAP-GED instantiations BP, BRANCH, BRANCH-FAST, and BRANCH-UNI. Further properties of rings and layers are summarized in Remark 2.

Remark 2 (Properties of Rings and Layers). Let $u \in V^G$ be a node and $\mathcal{R}_L(G, u) = ((N_l^G(u), OE_l^G(u), IE_l^G(u)))_{l=0}^{L-1}$ be the ring of size L rooted at u . Then the following statements follow from the involved definitions:

- 1) The node set $N_l^G(u)$ is empty if and only if $l > e_V^G(u)$, the edge set $IE_l^G(u)$ is empty if $l > e_V^G(u)$, and the edge set $OE_l^G(u)$ is empty if and only if $l > e_V^G(u) - 1$.
- 2) All node sets $N_l^G(u)$ and all edge sets $OE_l^G(u)$ and $IE_l^G(u)$ are disjoint.
- 3) The equalities $\bigcup_{l=0}^{L-1} N_l^G(u) = V^G$ and $\bigcup_{l=0}^{L-1} (OE_l^G(u) \cup IE_l^G(u)) = E^G$ hold for all $u \in V^G$ if and only if $L > \text{diam}(G)$.

4.2 Rings: Construction

Figure 5 shows how to construct a ring $\mathcal{R}_L(G, u)$ via breadth-first search. The algorithm maintains the level l of the currently processed layer along with the layer's node and edge sets N , OE , and IE , a vector \mathbf{d} that stores for each node $u' \in V^G$ the distance to the root u , flags $\text{discovered}[e]$ that indicate if the edge $e \in E^G$ has already been discovered by the algorithm, and a FIFO queue open which is initialized with the root u . Throughout the algorithm, $\mathbf{d}[u'] = d_V^G(u, u')$

Input: Graph G , node $u \in V^G$, constant $L \in \mathbb{N}_{>0}$.
Output: Ring $\mathcal{R}_L(G, u)$ rooted at u .

```

1  $l \leftarrow 0; N \leftarrow \emptyset; OE \leftarrow \emptyset; IE \leftarrow \emptyset;$ 
2  $\mathcal{R}_L(G, u) \leftarrow ((\emptyset, \emptyset, \emptyset)_l)_{l=0}^{L-1}; \text{open} \leftarrow \{u\};$ 
3  $d[u] \leftarrow 0; \text{for } u' \in V^G \setminus \{u\} \text{ do } d[u'] \leftarrow \infty;$ 
4 for  $e \in E^G$  do  $\text{discovered}[e] \leftarrow \text{false};$ 
5 while  $\text{open} \neq \emptyset$  do
6    $u' \leftarrow \text{open.pop}();$ 
7   if  $d[u'] > l$  then
8      $\mathcal{R}_L(G, u)_l \leftarrow (N, OE, IE); l \leftarrow l + 1;$ 
9      $N \leftarrow \emptyset; OE \leftarrow \emptyset; IE \leftarrow \emptyset;$ 
10   $N \leftarrow N \cup \{u'\};$ 
11  for  $(u', u'') \in E^G$  do
12    if  $\text{discovered}[(u', u'')] \text{ then continue};$ 
13     $\text{discovered}[(u', u'')] \leftarrow \text{true};$ 
14    if  $d[u''] = \infty$  then
15       $d[u''] \leftarrow l + 1;$ 
16      if  $d[u''] < L$  then  $\text{open.push}(u'');$ 
17    if  $d[u''] = l$  then  $IE \leftarrow IE \cup \{(u', u'')\};$ 
18    else  $OE \leftarrow OE \cup \{(u', u'')\};$ 
19  $\mathcal{R}_L(G, u)_l \leftarrow (N, OE, IE); \text{return } \mathcal{R}_L(G, u);$ 

```

Fig. 5. Construction of rings via breadth-first search.

holds for all nodes u' which have already been added to open, while newly discovered nodes u'' have $d[u''] = \infty$.

If a node u' is popped from open, we check if its distance is larger than the level l of the current layer. If this is case, we store the current layer, increment l , and clear the node and edge sets N , OE , and IE . Next, we add the node u' to the node set N and iterate through its undiscovered incident edges (u', u'') . We mark (u', u'') as discovered and push the node u'' to open if it has not been discovered yet and its distance to the root u is less than L . If this distance equals the level of the current layer, the edge (u', u'') is added to the inner edges IE ; otherwise, it is added to the outer edges OE . Once open is empty, the last layer is stored and the complete ring is returned. Since nodes and edges are processed at most once, the algorithm runs in $O(|V^G| + |E^G|)$ time and $O(|V^G|)$ space.

5 TWO RING BASED HEURISTICS

In this section, we present two new heuristics for ring based transformations to LSAPE. The heuristic RING uses the classical transformation strategy, the heuristic RING-ML employs our new machine learning based strategy.

5.1 RING: A Classical Instantiation of LSAPE-GED

RING is a classical instantiation of the paradigm LSAPE-GED which uses rings of size L as local structures. Therefore, what remains to be done is to define a distance measure $d_{\mathfrak{R}_L} : \mathfrak{R}_L \times \mathfrak{R}_L \rightarrow \mathbb{R}_{\geq 0}$ for the rings. We will define such a distance measure in a bottom-up fashion: Ring distances are defined in terms of layer distances, which, in turn, are defined in terms of node and edge set distances.

Assume that, for all pairs of graphs $(G, H) \in \mathfrak{G} \times \mathfrak{G}$, we have access to measures $d_{\mathcal{P}(V)}^{G,H} : \mathcal{P}(V^G) \times \mathcal{P}(V^H) \rightarrow \mathbb{R}_{\geq 0}$

and $d_{\mathcal{P}(E)}^{G,H} : \mathcal{P}(E^G) \times \mathcal{P}(E^H) \rightarrow \mathbb{R}_{\geq 0}$ that compute distances between subsets of nodes and edges. Then we can define a layer distance measure $d_{\mathfrak{L}}^{G,H} : \mathfrak{L}(G) \times \mathfrak{L}(H) \rightarrow \mathbb{R}_{\geq 0}$ as

$$d_{\mathfrak{L}}^{G,H}(\mathcal{L}^G, \mathcal{L}^H) := \frac{\alpha_0 d_{\mathcal{P}(V)}^{G,H}(N^G, N^H)}{\max\{|N^G|, |N^H|, 1\}} + \frac{\alpha_1 d_{\mathcal{P}(E)}^{G,H}(IE^G, IE^H)}{\max\{|IE^G|, |IE^H|, 1\}} + \frac{\alpha_2 d_{\mathcal{P}(E)}^{G,H}(OE^G, OE^H)}{\max\{|OE^G|, |OE^H|, 1\}},$$

where $\alpha \in \Delta^2$ is a simplex vector of weights associated to the distances between nodes, inner edges, and outer edges. We normalize by the sizes of the involved node and edge sets in order not to overrepresent large layers. Using the layer distances and a simplex weight vector $\lambda \in \Delta^{L-1}$, we define the ring distance measure $d_{\mathfrak{R}_L}$ as follows:

$$d_{\mathfrak{R}_L}((\mathcal{L}_l^G)_{l=0}^{L-1}, (\mathcal{L}_l^H)_{l=0}^{L-1}) := \sum_{l=0}^{L-1} \lambda_l d_{\mathfrak{L}}^{G,H}(\mathcal{L}_l^G, \mathcal{L}_l^H)$$

Next, we define node and edge set distances $d_{\mathcal{P}(V)}^{G,H}$ and $d_{\mathcal{P}(E)}^{G,H}$. To obtain tight upper bounds for GED, they should be defined such that $d_{\mathfrak{R}_L}(\mathcal{R}_L(G, u), \mathcal{R}_L(H, v))$ is small just in case the node assignment (G, H, u, v) induces a small edit cost. We suggest two strategies that meet this desideratum.

5.1.1 LSAPE Based Definitions of Node and Edge Set Distances

The first approach uses the edit cost functions c_V and c_E to populate LSAPE instances and then defines the distances in terms of the costs of optimal or greedy LSAPE solutions. Given node sets $N^G = \{u_1, \dots, u_{|N^G|}\} \subseteq V^G$ and $N^H = \{v_1, \dots, v_{|N^H|}\} \subseteq V^H$, an LSAPE instance $\mathbf{C} \in \mathbb{R}^{(|N^G|+1) \times (|N^H|+1)}$ is defined as

$$c_{i,k} := c_V(\ell_V^G(u_i), \ell_V^H(v_k)), \\ c_{i,|N^H|+1} := c_V(\ell_V^G(u_i), \epsilon), \text{ and} \\ c_{|N^G|+1,k} := c_V(\epsilon, \ell_V^H(v_k)),$$

for all $(i, k) \in [|N^G|] \times [|N^H|]$. Then, a solution $\pi \in \Pi(\mathbf{C})$ is computed—either optimally in $O(\min\{|N^G|, |N^H|\}^2 \max\{|N^G|, |N^H|\})$ time or greedily in $O(|N^G||N^H|)$ time—and the node set distance $d_{\mathcal{P}(V)}^{G,H}$ between N^G and N^H is defined as follows:

$$d_{\mathcal{P}(V)}^{G,H}(N^G, N^H) := \mathbf{C}(\pi)$$

The edge set distance $d_{\mathcal{P}(E)}^{G,H}$ can be defined analogously.

5.1.2 Multiset Intersection Based Definitions of Node and Edge Set Distances

Using LSAPE to define $d_{\mathcal{P}(V)}^{G,H}$ and $d_{\mathcal{P}(E)}^{G,H}$ yields fine-grained distance measures but incurs a relatively high computation time—especially, if optimal LSAPE solutions are computed. As an alternative, we suggest a faster, multiset intersection based approach which computes a proxy for the LSAPE

Input: Set of graphs \mathcal{G} , node and edge set distances

$d_{\mathcal{P}(V)}^{G,H}$ and $d_{\mathcal{P}(E)}^{G,H}$, tuning parameter μ .

Output: Optimized parameters L, α, λ .

- 1 $L \leftarrow 1 + \max_{G \in \mathcal{G}} |V^G|$;
- 2 build rings for all $G \in \mathcal{G}$ and all $u \in V^G$;
- 3 $L \leftarrow 1 + \max_{G \in \mathcal{G}} \text{diam}(G)$;
- 4 $(\alpha, \lambda) \leftarrow \arg \min \{f_{L,\mu}(\alpha, \lambda) \mid \alpha \in \Delta^2 \wedge \lambda \in \Delta^{L-1}\}$;
- 5 $L \leftarrow 1 + \max \text{supp}(\lambda)$;

Fig. 6. Algorithm for learning the parameters L, α , and λ .

based distances. For this, the distance between node sets $N^G \subseteq V^G$ and $N^H \subseteq V^H$ is defined as

$$\begin{aligned} d_{\mathcal{P}(V)}^{G,H} := & \delta_{|N^G| > |N^H|} \bar{c}_{del}(|N^G| - |N^H|) \\ & + \delta_{|N^G| < |N^H|} \bar{c}_{ins}(|N^H| - |N^G|) \\ & + \bar{c}_{sub}(\min\{|N^G|, |N^H|\} - |\ell_V^G[N^G] \cap \ell_V^H[N^H]|), \end{aligned}$$

where \bar{c}_{del} , \bar{c}_{ins} , and \bar{c}_{sub} are the average costs of deleting a node in N^G , inserting a node in N^H , and substituting a node in N^G by a differently labeled node in N^H , and $\ell_V^G[N^G]$ and $\ell_V^H[N^H]$ are the multiset images of N^G and N^H under the labelling functions ℓ_V^G and ℓ_V^H .

Since multiset intersections can be computed in quasilinear time [8], the dominant operation is the computation of \bar{c}_{sub} which requires $O(|N^G||N^H|)$ time. Again, the edge set distance $d_{\mathcal{P}(E)}^{G,H}$ can be defined analogously. The following Proposition 1 relates the LSAP based definitions of $d_{\mathcal{P}(V)}^{G,H}$ and $d_{\mathcal{P}(E)}^{G,H}$ to the ones based on multiset intersection and justifies our claim that the latter are proxies for the former.

Proposition 1 (Multiset Intersection Based Set Distances are Proxies for LSAP Based Distances). Let $G, H \in \mathfrak{G}$, $N^G \subseteq V^G$, $N^H \subseteq V^H$, and assume that c_V is quasimetric between N^G and N^H , i.e., that $c_V(\ell_V^G(u), \ell_V^H(v)) \leq c_V(\ell_V^G(u), \epsilon) + c_V(\epsilon, \ell_V^H(v))$ holds for all $(u, v) \in N^G \times N^H$. Then the definitions of $d_{\mathcal{P}(V)}^{G,H}(N^G, N^H)$ based on LSAP and multiset intersection incur the same number of node insertions, deletions, and substitutions. If, additionally, there are constants $c_{del}, c_{ins}, c_{sub} \in \mathbb{R}_{\geq 0}$ such that the equations $c_V(\ell_V^G(u), \ell_V^H(v)) = c_{sub}$, $c_V(\ell_V^G(u), \epsilon) = c_{del}$, and $c_V(\epsilon, \ell_V^H(v)) = c_{ins}$ hold for all $(u, v) \in N^G \times N^H$, the two definitions coincide. For the edge set distances $d_{\mathcal{P}(E)}^{G,H}$, analogous statements hold.

Proof: Assume w.l.o.g. that $|N^G| \leq |N^H|$, let \mathbf{C} be the LSAP instance for N^G and N^H constructed as shown in Section 5.1.1, and π be an optimal solution for \mathbf{C} . Since c_V is quasimetric, we know from [32] that π does not contain deletions and contains exactly $|N^H| - |N^G|$ insertions. This proves the first part of the proposition. If we additionally have constant edit costs between N^G and N^H , $\mathbf{C}(\pi)$ is reduced to the cost of $|N^H| - |N^G|$ insertions plus $c_{sub} = \bar{c}_{sub}$ times the number of non-identical substitutions. This last quantity is provided by $|N^G| - |\ell_V^G[N^G] \cap \ell_V^H[N^H]|$. We thus have $\mathbf{C}(\pi) = \bar{c}_{ins}(|N^H| - |N^G|) + \bar{c}_{sub}(|N^G| - |\ell_V^G[N^G] \cap \ell_V^H[N^H]|)$, as required. The proof for $d_{\mathcal{P}(E)}^{G,H}$ is analogous. \square

5.1.3 Choice of Parameters and Runtime Complexity

In Figure 6, an algorithm is described that, given a set of training graphs \mathcal{G} and node and edge set distances $d_{\mathcal{P}(V)}^{G,H}$ and $d_{\mathcal{P}(E)}^{G,H}$, learns good values for L, α , and λ . First, L is set to an upper bound for the ring sizes and all rings of size L rooted at the nodes of the graphs $G \in \mathcal{G}$ are constructed (cf. Figure 5). Next, L is lowered to 1 plus the largest $l < L$ such that there is a graph $G \in \mathcal{G}$ and a node $u \in V^G$ with $\mathcal{R}_L(G, u)_l \neq (\emptyset, \emptyset, \emptyset)$. Note that, by Remark 2, this l equals the maximal diameter of the graphs contained in \mathcal{G} . A blackbox optimizer [38] is then called to minimize

$$f_{L,\mu}(\alpha, \lambda) := \left[\mu + (1 - \mu) \left(\frac{|\text{supp}(\lambda)| - 1}{\max\{1, L - 1\}} \right) \right] \sum_{(G,H) \in \mathcal{G}^2} \text{RING}_{\alpha,\lambda,L}(G, H)$$

over all simplex vectors $\alpha \in \Delta^2$ and $\lambda \in \Delta^{L-1}$. $\text{RING}_{L,\alpha,\lambda}(G, H)$ is the upper bound for $\text{GED}(G, H)$ returned by RING if called with parameters L, α and λ ; and $\mu \in [0, 1]$ is a tuning parameter that should be small if one wants to optimize for tightness and large if one wants to optimize for runtime. We include $|\text{supp}(\lambda)| - 1$ in the objective, because only levels which are contained in the support of λ contribute to $d_{\mathcal{R}_L}$. Therefore, only few layer distances have to be computed if λ 's support is small. Once optimized parameters α and λ have been computed, L can be further lowered to $L = 1 + \max \text{supp}(\lambda)$.

Remark 3 (Runtime Complexity of RING). Let $G, H \in \mathfrak{G}$ be graphs, $L \in \mathbb{N}_{\geq 0}$ be a constant, and Ω be the size of the largest node or edge set contained in one of the rings of G and H . Then, once all rings have been constructed, RING requires $O(\Omega^3 |V^G| |V^H|)$ time to populate its LSAP instance \mathbf{C} if LSAP based node and edge set distances are used, and $O(\Omega^2 |V^G| |V^H|)$ time if multiset intersection based distances are employed.

5.2 RING-ML: A Machine Learning Based Instantiation of LSAP-GED

If LSAP-GED is instantiated with the help of machine learning techniques, feature vectors associated to the node assignments have to be defined. The heuristic RING-ML uses rings of size L to accomplish this task. Formally, RING-ML defines a function $\mathcal{F} : \mathfrak{A} \rightarrow \mathbb{R}^{6L+10}$ that maps node assignments to feature vectors with six features per layer and ten global features. Let $(G, H, u, v) \in \mathfrak{A}$ be a node assignment and $\mathcal{R}_L(G, u)$ and $\mathcal{R}_L(H, v)$ be the rings rooted at u in G and at v in H , respectively. For each level $l \in \{0, \dots, L-1\}$, a feature vector $\mathbf{x}^l \in \mathbb{R}^6$ is constructed by comparing the layers $\mathcal{R}_L(G, u)_l = (N_l^G(u), OE_l^G(u), IE_l^G(u))$ and $\mathcal{R}_L(H, v)_l = (N_l^H(v), OE_l^H(v), IE_l^H(v))$ at level l :

$$\begin{aligned} \mathbf{x}_0^l &:= |N_l^G(u)| - |N_l^H(v)| \\ \mathbf{x}_1^l &:= |OE_l^G(u)| - |OE_l^H(v)| \\ \mathbf{x}_2^l &:= |IE_l^G(u)| - |IE_l^H(v)| \\ \mathbf{x}_3^l &:= d_{\mathcal{P}(V)}^{G,H}(N_l^G(u), N_l^H(v)) \\ \mathbf{x}_4^l &:= d_{\mathcal{P}(E)}^{G,H}(OE_l^G(u), OE_l^H(v)) \\ \mathbf{x}_5^l &:= d_{\mathcal{P}(E)}^{G,H}(IE_l^G(u), IE_l^H(v)) \end{aligned}$$

TABLE 2
Properties of Datasets

dataset	avg.(max.) $ V^G $	avg.(max.) $ E^G $	classes
AIDS	15.7(95)	16.2(103)	2
LETTER	4.7(9)	4.5(9)	15
PAH	20.7(28)	24.4(34)	2
ALKANE	8.9(10)	7.9(9)	1

The first three features compare the layers’ topologies. The last three features use node and edge set distances $d_{\mathcal{P}(V)}^{G,H}$ and $d_{\mathcal{P}(E)}^{G,H}$ to express the similarity of the involved node and edge labels. RING-ML also constructs a vector $\mathbf{x}^{G,H} \in \mathbb{R}^{10}$ of ten global features: the number of nodes and edges of G and H , the average costs for deleting nodes and edges from G , the average costs for inserting nodes and edges into H , and the average costs for substituting nodes and edges in G by nodes and edges in H . The complete feature vector $\mathcal{F}(G, H, u, v)$ is then defined as the concatenation of the global features $\mathbf{x}^{G,H}$ and the layer features \mathbf{x}^L .

Remark 4 (Runtime Complexity of RING-ML). Let $G, H \in \mathcal{G}$ be graphs, $L \in \mathbb{N}_{\geq 0}$ be a constant, and Ω be the size of the largest node or edge set contained in one of the rings of G and H . Then, once all rings have been constructed, RING-ML requires $O((\Omega^3 + f^{\text{ML}}(1))|V^G||V^H|)$ time to populate its LSAP instance \mathbf{C} if LSAP based node and edge set distances are used, and $O((\Omega^2 + f^{p^*}(1))|V^G||V^H|)$ time if multiset intersection based distances are employed. $O(f^{p^*}(n))$ is the complexity of evaluating the probability estimate p^* of the chosen machine learning technique on feature vectors of size n .

6 EXPERIMENTAL EVALUATION

6.1 Datasets and Compared Methods

We tested on the benchmark datasets PAH, ALKANE, LETTER, and AIDS [35], which are widely used in the research community [10], [11], [12], [13], [14], [17], [23], [24], [26], [34]. Table 2 summarizes some of their properties. LETTER contains graphs that model highly distorted letter drawings, while the graphs in PAH, ALKANE, and AIDS represent chemical compounds. For LETTER, we used the edit costs suggested in [28], for PAH, ALKANE, and AIDS the edit costs defined in [29]. The graphs contained PAH and ALKANE have unlabeled nodes, i. e., PAH and ALKANE contain graphs whose information is exclusively encoded in the topologies. On the contrary, the graphs contained in LETTER and AIDS have many different node labels. We also carried out tests on synthetic datasets to evaluate the effect of the node informativeness in a controlled setting. These datasets are described in Section 6.4.4 below.

We tested three variants of RING: RING^{OPT} uses optimal LSAP for defining the set distances $d_{\mathcal{P}(V)}^{G,H}$ and $d_{\mathcal{P}(E)}^{G,H}$, RING^{GD} uses greedy LSAP, and RING^{MS} uses the multiset intersection based approach. RING-ML was tested with three different machine learning techniques: SVCs with RBF kernel and probability estimates [18], fully connected feedforward DNNs [19], and 1-SVMs with RBF kernel. We compared to competitors that can cope with non-uniform edit costs: BP, BRANCH, BRANCH-FAST, SUBGRAPH, WALKS,

and PREDICT. As WALKS assumes constant edit costs, we slightly extended it by averaging the costs before each run. To handle SUBGRAPH’s exponential complexity, we set a time limit of 1 ms for computing a cell $c_{i,k}$ of its LSAP instance \mathbf{C} . PREDICT was tested with the same probability estimates as RING-ML. Since some of our test graphs have symbolic labels and not all of them are of the same size, we did not include NGM. For all methods, we varied the number of threads and the maximal number of LSAP solutions over the set $\{1, 4, 7, 10\}$ and parallelized the construction of \mathbf{C} .

6.2 Choice of Meta-Parameters and Training of Machine Learning Based Methods

For learning the meta-parameters of RING^{OPT}, RING^{GD}, RING^{MS}, SUBGRAPH, and WALKS, and training the DNNs, the SVCs, and the 1-SVMs, we picked a training set $\mathcal{S}_1 \subset \mathcal{D}$ with $|\mathcal{S}_1| = 50$ for each dataset \mathcal{D} . Following [14], [15], we learned the parameter L of the methods SUBGRAPH and WALKS by minimizing the average upper bound on \mathcal{S}_1 over $L \in \{1, 2, 3, 4, 5\}$. For choosing the meta-parameters of the variants of RING, we set the tuning parameter μ to 1 and initialized our blackbox optimizer with 100 randomly constructed simplex vectors α and λ . For determining the network structure of the fully connected feedforward DNNs, we carried out 5-fold cross validation, varying the number of hidden layers, the number of neurons per hidden layers, and the activation function at hidden layers over the grid $\{1, \dots, 10\} \times \{1, \dots, 20\} \times \{\text{ReLU}, \text{Sigmoid}\}$. Similarly, we determined the meta-parameters C and γ of the SVC via 5-fold cross-validation on the grid $\{10^{-3}, \dots, 10^3\} \times \{10^{-3}, \dots, 10^3\}$. For the 1-SVM, we set the meta-parameter γ to $1/\dim(\mathcal{F})$, where $\dim(\mathcal{F})$ is the dimensionality of the feature vectors. We used mIPFP [24] to compute close to optimal node maps $\pi \in \Pi(G, H)$ for all $(G, H) \in \mathcal{S}_1 \times \mathcal{S}_1$. To ensure that the training data \mathcal{T} used by DNN and SVC is balanced, we randomly picked only $|\pi|$ node assignments $(u, v) \notin \pi$ for each node map π .

6.3 Protocol, Test Metrics, and Implementation

For each dataset \mathcal{D} , we randomly selected a test set $\mathcal{S}_2 \subseteq \mathcal{D} \setminus \mathcal{S}_1$ with $|\mathcal{S}_2| = \min\{100, |\mathcal{D} \setminus \mathcal{S}_1|\}$, and ran each method on each pair $(G, H) \in \mathcal{S}_2 \times \mathcal{S}_2$ with $G \neq H$. We recorded the average runtime in seconds (t), the average value of the returned upper bound for GED (b), and the ratio of graphs which are correctly classified if the returned upper bound is employed in combination with a 1-NN classifier (r).

All methods were implemented in C++. We employed the LSAP solver [32], used NOMAD [39] as our blackbox optimizer, LIBSVM [40] for implementing SVCs and 1-SVMs, and FANN [41] for implementing DNNs. Tests were run on a machine with two Intel Xeon E5-2667 v3 processors with 8 cores each and 98 GB of main memory. Sources and datasets are available at <https://github.com/dbblumenthal/gedlib/>.

6.4 Results of the Experiments

6.4.1 Effect of Machine Learning Techniques

Table 3 shows the performances of different machine learning techniques when used in combination with the feature vectors defined by RING-ML and PREDICT on the datasets

TABLE 3
Effect of Machine Learning Techniques on RING-ML and PREDICT

	b	t	r
LETTER			
<i>feature vectors</i>	RING-ML [this paper]		
DNN [19]	8.24	$2.99 \cdot 10^{-4}$	0.20
SVC [18]	5.68	$6.47 \cdot 10^{-3}$	0.73
1-SVM [this paper]	6.07	$2.58 \cdot 10^{-3}$	0.81
<i>feature vectors</i>	PREDICT [18]		
DNN [19]	8.19	$1.48 \cdot 10^{-4}$	0.22
SVC [18]	5.22	$2.82 \cdot 10^{-3}$	0.76
1-SVM [this paper]	6.07	$2.07 \cdot 10^{-3}$	0.81
PAH			
<i>feature vectors</i>	RING-ML [this paper]		
DNN [19]	25.29	$5.69 \cdot 10^{-3}$	0.65
SVC [18]	31.91	$7.19 \cdot 10^{-1}$	0.62
1-SVM [this paper]	24.55	$2.12 \cdot 10^{-1}$	0.71
<i>feature vectors</i>	PREDICT [18]		
DNN [19]	44.03	$1.23 \cdot 10^{-3}$	0.56
SVC [18]	36.68	$3.40 \cdot 10^{-1}$	0.65
1-SVM [this paper]	24.55	$1.14 \cdot 10^{-1}$	0.71

LETTER and PAH (with number of threads and maximal number of LSAPE solutions set to 10). The results for ALKANE and AIDS are similar and are omitted because of space constraints. The tightest upper bounds and best classification ratios were achieved by 1-SVMs. Using DNNs improved the runtime, but resulted in dramatically worse classification ratios and upper bounds. Using SVCs instead of 1-SVMs negatively affected all three test metrics. In the following, we therefore only report the results for 1-SVMs and DNNs.

6.4.2 Effect of Number of Threads and Maximal Number of LSAPE Solutions

Figure 7 shows the effects of varying the number of threads and the maximal number of LSAPE solutions. Unsurprisingly, slower methods benefited more from parallelization than faster ones. The only exception is WALKS, whose local structure distances require a lot of unparallelizable pre-computing. Computing more than one LSAPE solution tightened the upper bounds of mainly those methods that yielded loose upper bounds if run with only one solution. The outlier of SUBGRAPH on LETTER is due to the fact that SUBGRAPH was run with a time limit on the computation of the subgraph distances; and that the algorithm used for solving these subproblems is guaranteed to always return the same value only if it is run to optimality. Also note that increasing the maximal number of LSAPE solutions significantly increased the runtimes of only the fastest algorithms. This is because computationally expensive LSAPE-GED instantiations spend most of the runtime on constructing their LSAPE instances. For these methods, the additional time required to enumerate the LSAPE solutions hence turned out to be negligible.

6.4.3 Overall Performance on Benchmark Datasets

Figure 8 summarizes the overall performances of the compare methods on the four datasets with the number of threads and maximal number of LSAPE solutions fixed to 10. We

see that, across all datasets, RING^{OPT} yielded the tightest upper bound of all tested methods. RING^{MS}, i. e., the variant of RING which uses the multiset intersection based approach for computing the layer distances, performed excellently, too, as it was significantly faster than RING^{OPT} and yielded only slightly looser upper bounds. On the contrary, using a greedy, suboptimal LSAPE solver for computing the layer distances as done by RING^{GD} turned out not to be a good idea, as doing so did not significantly reduce the runtimes and led to much looser upper bounds on the datasets LETTER and AIDS. Note that on the datasets PAH and ALKANE, the tightness gaps between the baseline approaches BP, BRANCH, and BRANCH-FAST and the methods that use rings, subgraphs or walks to capture more topological information turned out to be much more significant than on LETTER and AIDS. Cf. Section 6.4.4 below for an explanation.

If run with 1-SVMs with RBF kernels, the machine learning based methods PREDICT and RING-ML performed very similarly in terms of classification ratio and tightness of the produced upper bounds. Both methods yielded very promising classification ratios on the datasets PAH and LETTER. Running RING-ML and PREDICT with DNNs instead of 1-SVMs dramatically improved the runtimes but led to looser upper bounds and worse classification ratios. If run with DNNs, RING-ML produced tighter upper bounds than PREDICT. Yet, globally, the machine learning based methods were outperformed by classical LSAPE-GED instantiations.

6.4.4 Effect of Node Informativeness

As mentioned in the previous section, methods such as the variants of RING that use enlarged local structures performed much better on PAH and ALKANE than on LETTER and AIDS. The natural explanation for this is that while PAH and ALKANE contain unlabeled graphs whose information is entirely encoded in the topology, the graphs contained in LETTER and AIDS have labels on the nodes and hence a higher node informativeness. Together with the hypothesis that instances of LSAPE-GED benefit more from considering enlarged local structures if the information mainly resides in the graphs' topologies, this explains the observed results.

To test this hypothesis, i. e., evaluate whether a small node informativeness indeed correlates with a large tightness gap between the upper bounds produced by LSAPE-GED instantiations that use, respectively, narrow and enlarged local structures, we ran additional experiments on synthetic datasets S-MOL-1, S-MOL-4, S-MOL-7, and S-MOL-10. These datasets contain "synthetic molecules" which are similar to the ones contained in ALKANE and hence allow to employ the same edit costs [29]. More precisely, we generated the molecules as pairwise non-isomorphic trees whose sizes were randomly drawn from $\{8, 9, 10, 11, 12\}$. Next, we generated four variants of each molecule—one for each of the four datasets S-MOL-1, S-MOL-4, S-MOL-7, and S-MOL-10—by randomly drawing node labels from node label alphabets $\Sigma_V = [1]$, $\Sigma_V = [4]$, $\Sigma_V = [7]$, and $\Sigma_V = [10]$, respectively. Edges are unlabeled in all variants. Hence, in the dataset S-MOL-1, the information exclusively resides in the graphs' topologies, whereas the graphs contained in S-MOL-10 have a lot of information on the nodes. The datasets S-MOL-4 and S-MOL-7 assume intermediate positions.

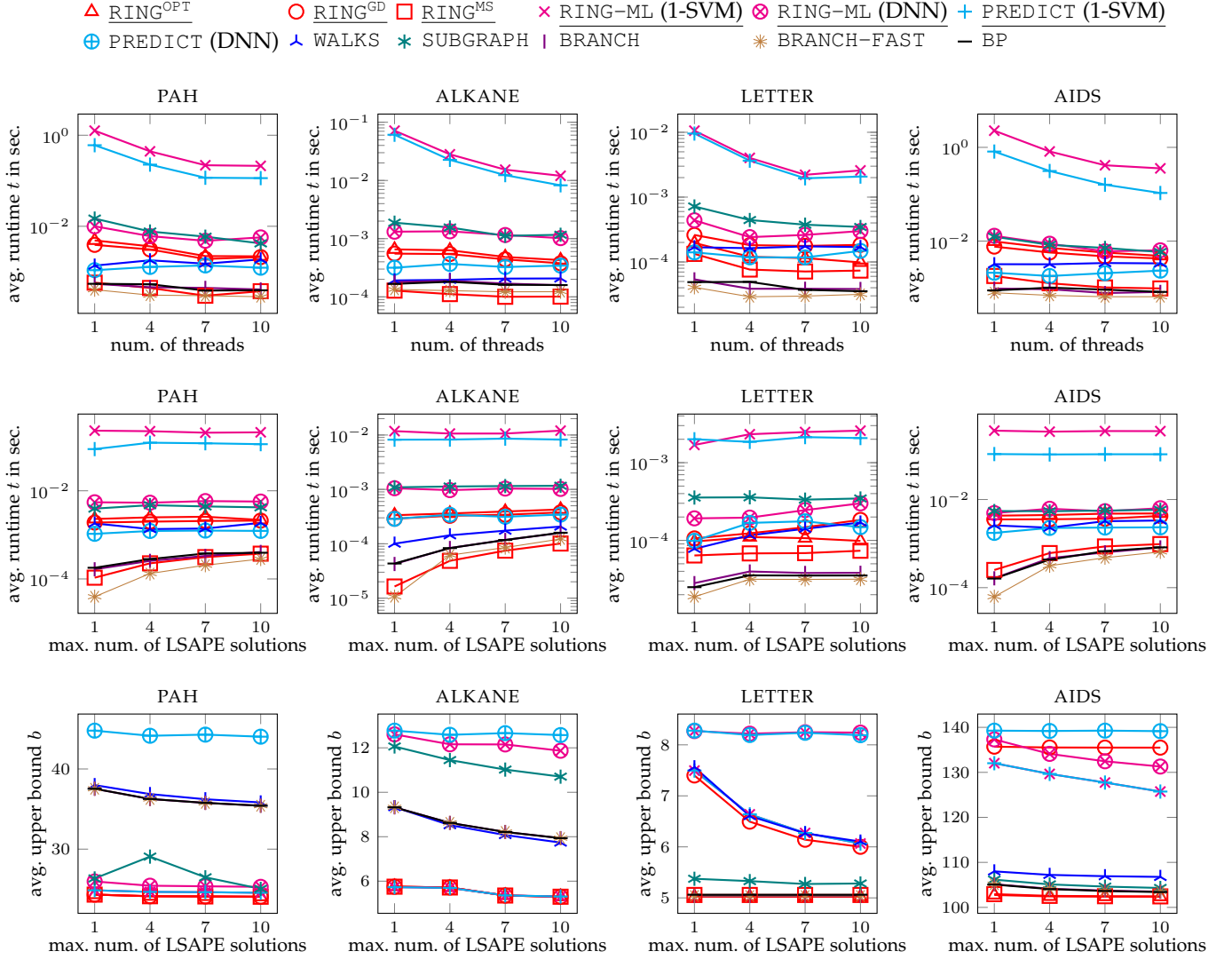


Fig. 7. Number of threads vs. runtimes (first row, maximal number of LSAP solutions fixed to 10) and maximal number of LSAP solutions vs. runtimes and upper bounds (second and third row, number of threads fixed to 10). Underlined methods use techniques proposed in this paper.

We then ran the protocol described in Section 6.3 on all four datasets and, for each dataset and algorithm, computed the deviation

$$d(\text{ALG}) := 100(b(\text{ALG}) - \min_{\text{ALG}'} b(\text{ALG}') / (\min_{\text{ALG}'} b(\text{ALG}'))$$

in percent from the algorithm which yielded the tightest average upper bound on the dataset. Note that, with this definition, we have $d(\text{ALG}) = 0$ for the algorithm ALG that produced the tightest average upper bound.

Figure 9 shows the results of the experiments. To improve the readability of the plot, we only show the curves for RING^{OPT} , RING^{MS} , and the methods BP, BRANCH, and BRANCH-FAST that employ narrow local structures. All other methods produced significantly looser upper bounds. We see that RING^{OPT} and RING^{MS} performed very similarly and always yielded the best upper bounds. Moreover, the tightness gap between RING^{OPT} and RING^{MS} , on the one side, and BP, BRANCH, and BRANCH-FAST, on the other side, turned out to be much higher on the dataset S-MOL-1 than on the datasets S-MOL-4, S-MOL-7, and S-MOL-10, whose graphs

have more information on the nodes. Our experiments on synthetic graphs hence confirmed the hypothesis we extrapolated from the results for PAH, ALKANE, LETTER, and AIDS: Using enlarged local structures such as rings is especially beneficial if most information resides in the graphs' topologies and little information on the nodes is available.

6.4.5 Upshot of the Results

The experimental results lead us to four takeaway messages: First, if one wants to use instantiations of LSAP-GED for computing tight upper bounds for GED on graphs where most information is encoded in the topology, the newly proposed algorithms RING^{OPT} and RING^{MS} are the best choices. Second, it is always a good idea to increase the number of LSAP solutions as suggested in this paper. Doing so only slightly increases the runtime and at the same time significantly improves the upper bounds of methods that yield loose upper bounds if run with only one LSAP solution. Third, machine learning based LSAP-GED instantiations such as RING-ML and PREDICT should be run with 1-SVMs as suggested in this paper if one wants to optimize

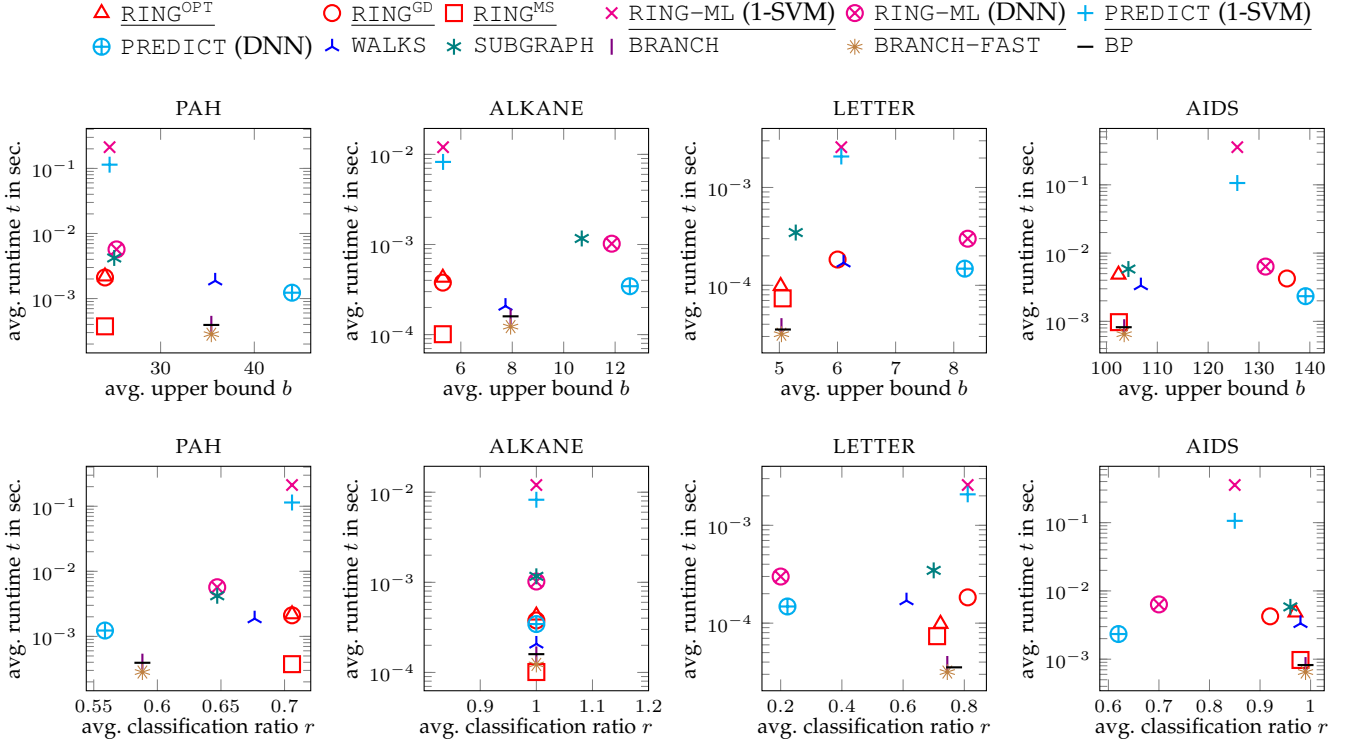


Fig. 8. Runtimes vs. upper bounds and classification ratios with number of threads and maximal number of LSAPE solutions fixed to 10. Underlined methods use techniques proposed in this paper. As ALKANE contains only one graph class, on this dataset, we have $r(\text{ALG}) = 1$ for all algorithms ALG.

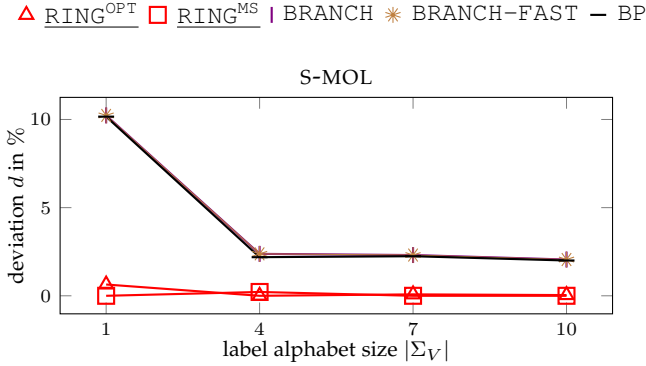


Fig. 9. Effect of node informativeness with number of threads and maximal number of LSAPE solutions fixed to 10. Underlined methods use techniques proposed in this paper. Methods whose curves are not displayed yielded higher deviations.

for classification ratio and tightness of the produced upper bound, and with DNNs as suggested in [19] if one wants to optimize for runtime behaviour. Fourth, RING-ML and PREDICT show promising potential but cannot yet compete with classical instantiations of LSAPE-GED. If run with 1-SVMs, they are competitive in terms of quality (classification ratio and tightness of the produced upper bound) but not in terms of runtime; if run with DNNs, the opposite is the case. The open challenge for future work is therefore to develop new machine learning frameworks that exploit the information encoded in RING-ML's and PREDICT's feature vectors such that the resulting GED heuristics are competitive both w. r. t. quality and w. r. t. runtime behaviour.

7 SUMMARY

In this paper, we formalized the paradigm LSAPE-GED for upper bounding GED via transformations to LSAPE and showed how to use machine learning in general in 1-SVMs in particular for this purpose. Moreover, we introduced rings, a new kind of local structures to be used by instantiations of LSAPE-GED, and presented the algorithms RING and RING-ML that use rings to instantiate LSAPE-GED in a classical way (RING) or via machine learning (RING-ML). Extensive experiments showed that, on datasets where the information is mainly encoded in the graphs' topologies, the proposed techniques clearly outperform the state of the art.

REFERENCES

- [1] P. Foggia, G. Percannella, and M. Vento, "Graph matching and learning in pattern recognition in the last 10 years," *Int. J. Pattern Recognit. Artif. Intell.*, vol. 28, no. 1, pp. 1450001:1–1450001:40, 2014.
- [2] M. Vento, "A long trip in the charming world of graphs for pattern recognition," *Pattern Recognit.*, vol. 48, no. 2, pp. 291–301, 2015.
- [3] M. Stauffer, T. Tschachtli, A. Fischer, and K. Riesen, "A survey on applications of bipartite graph edit distance," in *GbRPR*, 2017, pp. 242–252.
- [4] M. Stauffer, A. Fischer, and K. Riesen, "A novel graph database for handwritten word images," in *S+SSPR*, 2016, pp. 553–563.
- [5] E. Ozdemir and C. Gunduz-Demir, "A hybrid classification model for digital pathology using structural and statistical pattern recognition," *IEEE Trans. Med. Imaging*, vol. 32, no. 2, pp. 474–483, 2013.
- [6] H. Bunke and G. Allermann, "Inexact graph matching for structural pattern recognition," *Pattern Recognit. Lett.*, vol. 1, no. 4, pp. 245–253, 1983.
- [7] D. Justice and A. Hero, "A binary linear programming formulation of the graph edit distance," *IEEE Trans. Pattern Anal. Mach. Intell.*, vol. 28, no. 8, pp. 1200–1214, 2006.

- [8] Z. Zeng, A. K. H. Tung, J. Wang, J. Feng, and L. Zhou, "Comparing stars: On approximating graph edit distance," *Proc. VLDB Endow.*, vol. 2, no. 1, pp. 25–36, 2009.
- [9] C.-L. Lin, "Hardness of approximating graph transformation problem," in *Algorithms and Computation*, 1994, pp. 74–82.
- [10] D. B. Blumenthal and J. Gamper, "On the exact computation of the graph edit distance," *Pattern Recognit. Lett.*, 2018, in press.
- [11] K. Riesen and H. Bunke, "Approximate graph edit distance computation by means of bipartite graph matching," *Image Vis. Comput.*, vol. 27, no. 7, pp. 950–959, 2009.
- [12] W. Zheng, L. Zou, X. Lian, D. Wang, and D. Zhao, "Efficient graph similarity search over large graph databases," *IEEE Trans. Knowl. Data Eng.*, vol. 27, no. 4, pp. 964–978, 2015.
- [13] D. B. Blumenthal and J. Gamper, "Improved lower bounds for graph edit distance," *IEEE Trans. Knowl. Data Eng.*, vol. 30, no. 3, pp. 503–516, 2018.
- [14] V. Carletti, B. Gaüzère, L. Brun, and M. Vento, "Approximate graph edit distance computation combining bipartite matching and exact neighborhood substructure distance," in *GbRPR*, 2015, pp. 188–197.
- [15] B. Gaüzère, S. Bougleux, K. Riesen, and L. Brun, "Approximate graph edit distance guided by bipartite matching of bags of walks," in *S+SSPR*, 2014, pp. 73–82.
- [16] K. Riesen, H. Bunke, and A. Fischer, "Improving graph edit distance approximation by centrality measures," in *ICPR*, 2014, pp. 3910–3914.
- [17] F. Serratos and X. Cortés, "Graph edit distance: Moving from global to local structure to solve the graph-matching problem," *Pattern Recognit. Lett.*, vol. 65, pp. 204–210, 2015.
- [18] K. Riesen and M. Ferrer, "Predicting the correctness of node assignments in bipartite graph matching," *Pattern Recognit. Lett.*, vol. 69, pp. 8–14, 2016.
- [19] X. Cortés, D. Conte, H. Cardot, and F. Serratos, "A deep neural network architecture to estimate node assignment costs for the graph edit distance," in *S+SSPR*, 2018, pp. 326–336.
- [20] K. Riesen and H. Bunke, "Improving bipartite graph edit distance approximation using various search strategies," *Pattern Recognit.*, vol. 48, no. 4, pp. 1349–1363, 2015.
- [21] M. Ferrer, F. Serratos, and K. Riesen, "A first step towards exact graph edit distance using bipartite graph matching," in *GbRPR*, 2015, pp. 77–86.
- [22] K. Riesen, A. Fischer, and H. Bunke, "Improved graph edit distance approximation with simulated annealing," in *GbRPR*, 2017, pp. 222–231.
- [23] S. Bougleux, L. Brun, V. Carletti, P. Foggia, B. Gaüzère, and M. Vento, "Graph edit distance as a quadratic assignment problem," *Pattern Recognit. Lett.*, vol. 87, pp. 38–46, 2017.
- [24] É. Daller, S. Bougleux, B. Gaüzère, and L. Brun, "Approximate graph edit distance by several local searches in parallel," in *ICPRAM*, 2018, pp. 149–158.
- [25] N. Boria, S. Bougleux, and L. Brun, "Approximating GED using a stochastic generator and multistart IPFP," in *S+SSPR*, 2018, pp. 460–469.
- [26] D. B. Blumenthal, É. Daller, S. Bougleux, L. Brun, and J. Gamper, "Quasimetric graph edit distance as a compact quadratic assignment problem," in *ICPR*, 2018, pp. 934–939.
- [27] D. B. Blumenthal, S. Bougleux, J. Gamper, and L. Brun, "Ring based approximation of graph edit distance," in *S+SSPR*, 2018, pp. 293–303.
- [28] K. Riesen and H. Bunke, *Graph Classification and Clustering Based on Vector Space Embedding*. Singapore: World Scientific, 2010.
- [29] Z. Abu-Aisheh, B. Gaüzère, S. Bougleux, J.-Y. Ramel, L. Brun, R. Raveaux, P. Héroux, and S. Adam, "Graph edit distance contest 2016: Results and future challenges," *Pattern Recognit. Lett.*, vol. 100, pp. 96–103, 2017.
- [30] K. Riesen, *Structural Pattern Recognition with Graph Edit Distance*. Cham: Springer, 2015.
- [31] S. Bougleux, B. Gaüzère, and L. Brun, "Graph edit distance as a quadratic program," in *ICPR*, 2016, pp. 1701–1706.
- [32] S. Bougleux, B. Gaüzère, D. B. Blumenthal, and L. Brun, "Fast linear sum assignment with error-correction and no cost constraints," *Pattern Recognit. Lett.*, 2018, in press.
- [33] T. Uno, "A fast algorithm for enumerating bipartite perfect matchings," in *ISAAC*, 2001, pp. 367–379.
- [34] K. Riesen, M. Ferrer, A. Fischer, and H. Bunke, "Approximation of graph edit distance in quadratic time," in *GbRPR*, 2015, pp. 3–12.
- [35] K. Riesen and H. Bunke, "IAM graph database repository for graph based pattern recognition and machine learning," in *S+SSPR*, 2008, pp. 287–297.
- [36] H.-T. Lin, C.-J. Lin, and R. C. Weng, "A note on Platt's probabilistic outputs for support vector machines," *Mach. Learn.*, vol. 68, no. 3, pp. 267–276, 2007.
- [37] B. Schölkopf, J. C. Platt, J. Shawe-Taylor, A. J. Smola, and R. C. Williamson, "Estimating the support of a high-dimensional distribution," *Neural Comput.*, vol. 13, no. 7, pp. 1443–1471, 2001.
- [38] L. M. Rios and N. V. Sahinidis, "Derivative-free optimization: a review of algorithms and comparison of software implementations," *J. Global Optim.*, vol. 56, no. 3, pp. 1247–1293, 2013.
- [39] S. Le Digabel, "Algorithm 909: Nomad: Nonlinear optimization with the mads algorithm," *ACM Trans. Math. Softw.*, vol. 37, no. 4, pp. 44:1–44:15, 2011.
- [40] C.-C. Chang and C.-J. Lin, "LIBSVM: A library for support vector machines," *ACM Trans. Intell. Syst. Technol.*, vol. 2, no. 3, p. 27, 2011.
- [41] S. Nissen, "Implementation of a fast artificial neural network library (FANN)," Department of Computer Science, University of Copenhagen, Tech. Rep., 2003. [Online]. Available: <http://fann.sourceforge.net/report/>



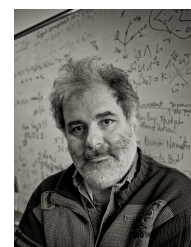
David B. Blumenthal is a Ph. D. student at the Faculty of Computer Science of the Free University of Bozen-Bolzano, Italy. His main interests are graph edit distance and graph similarity search. He holds Master's degrees in Mathematics and Philosophy from the TU Berlin and the FU Berlin.



Sébastien Bougleux is an associate professor at UNICAEN, ENSICAEN, CNRS, GREYC, Normandie Université, Caen, France. His main interests are image processing and analysis as well as graph matching and graph similarity search. He holds a Ph. D. degree in Computer Science from the Université de Caen Normandie.



Johann Gamper is a full professor at the Faculty of Computer Science of the Free University of Bozen-Bolzano. His main interests are database technologies for processing temporal and spatial data, data warehousing, and approximate query answering. He holds a Ph. D. degree in Computer Science from the RWTH Aachen.



Luc Brun is a full professor at ENSICAEN, CNRS, GREYC, Normandie Université, Caen, France. His main research interests are color image segmentation, combinatorial maps, pyramidal data structures, and metrics on graphs. He holds a Ph. D. degree in Computer Science from the Université Bordeaux I.